THE STRANGENESS AND CHARM OF DENSE NUCLEAR MATTER*

Peter Senger

Gesellschaft für Schwerionenforschung (GSI)
Postfach 110552, 64220 Darmstadt, Germany

(Received December 28, 2001)

The creation of strangeness and charm in nucleus–nucleus collisions at threshold beam energies is discussed as a probe for compressed baryonic matter. Experimental data on strangeness production at SIS energies indicate that the properties of kaons and antikaons are modified in dense nuclear matter. An experiment is proposed at the future GSI facility to explore the QCD phase diagram in the region of highest baryon densities. An important observable will be charm production close to threshold.

PACS numbers: 25.75.Dw

1. Introduction

The goal of the nuclear reaction program at the present and the future GSI accelerators is to investigate the properties of highly compressed nuclear matter. Such a form of matter exists in various so far unexplored phases in the interior of neutron stars and in the core of supernova explosions. Fig. 1 illustrates structures of neutron stars as proposed by various models (compilation by Weber [1]). Novel phases of subatomic matter are expected to exist in the core of neutron stars — each having their own nuclear equation-of-state.

Further progress needs information on the chemistry of quarks and hadrons at high densities, in particular for strange particles. The chemical potentials of hadrons depend strongly on the in-medium properties of these particles. It is of crucial importance to know at which baryon density the hadrons dissolve into quarks and gluons and how the masses of the particles are modified in the different phases of strongly interacting matter. Experiments using heavy ion accelerators are performed world-wide in order to obtain such information. The melting of hadrons into quarks and gluons

* Presented at the XXVII Mazurian Lakes School of Physics, Krzyże, Poland, September 2–9, 2001.

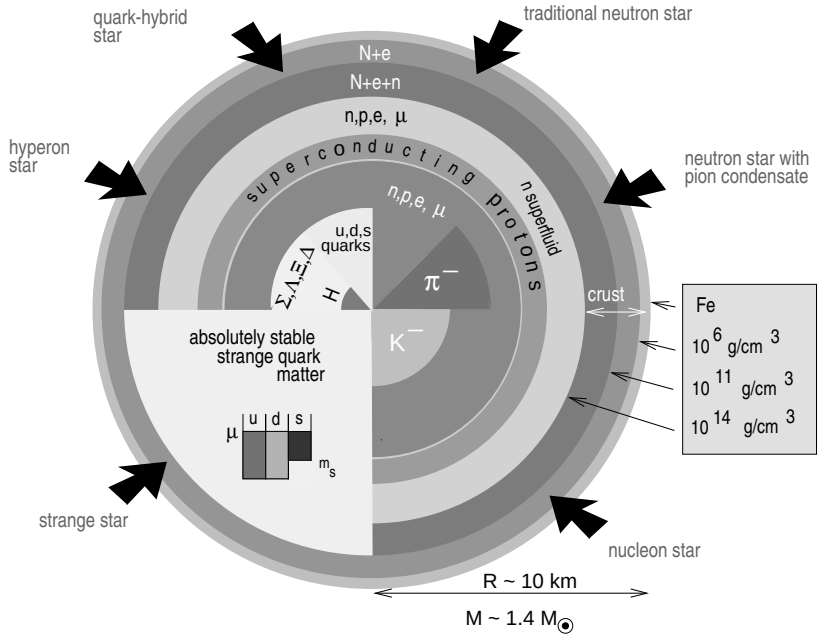

Fig. 1. Structures of neutron stars and novel phases of subatomic matter as predicted by different models (taken from [1]).

at high densities explores the phenomenon of confinement, one of the most fascinating features of strong interaction physics. The theory of strong interaction, Quantum Chromo Dynamics (QCD), predicts a deconfinement phase transition at a temperature around 170 MeV at zero net baryon density. Calculations for low temperatures and finite baryon densities, however, are largely uncertain. Hence, a quantitative understanding of confinement is still lacking.

Another enigma of QCD is the origin of hadron masses. Why is a hadron, that is composed of light quarks, much heavier than the sum of the masses of its constituents? (This question is not to be confused with the generation of masses of quarks and leptons by the Higgs-field.) The question of hadron masses is closely related to chiral symmetry, a fundamental property of QCD in the limit of vanishing quark masses (see also the contribution by V. Metag). During the first few microseconds after the Big Bang the Universe went through a phase transition where the quarks and gluons were confined into hadrons. Simultaneously, the original chiral symmetry was spontaneously broken. At high temperatures or at high baryon densities, however, chiral symmetry is expected to be at least partially restored.

Hence, the experimental investigation of hadron properties in hot and dense matter provides an access to this symmetry breaking mechanism and to the origin of hadron masses.

In the laboratory hadronic matter can be generated in a wide range of temperatures and densities by colliding atomic nuclei at high energies. For a very short time highly compressed nuclear matter is formed in the collision zone. The time evolution of the baryon densities during the course of central collisions between two gold nuclei at different beam energies is depicted in Fig. 2 which shows the results of a transport calculation [2]. A major fraction

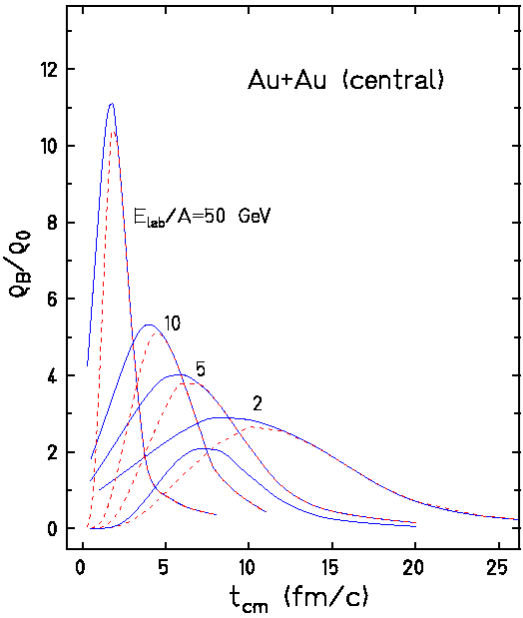

Fig. 2. Baryon density as function of time for central Au+Au collisions (full lines). The dashed lines represent the density of baryons which underwent at least one collision (taken from [2]).

of the energy of motion of the two nuclei is converted into heat, *i.e.* chaotic motion of the nucleons corresponding to a finite temperature. If the energy pumped into the collision zone is sufficiently high the quark–gluon substructure of nucleons becomes relevant. At first nucleons are excited to short lived states (baryonic resonances, composites with 3 quarks) which decay by the emission of mesons (quark–antiquark pairs). This mixture of nucleons, baryons and mesons, all strongly interacting particles (and antiparticles), is generally called hadronic matter, or baryonic matter if baryons prevail. At even higher temperatures the hadrons melt, and the constituents, the quarks and gluons, can move freely forming a new phase, the Quark–Gluon–Plasma.

2. Strange mesons in dense baryonic matter

Strange mesons are regarded as promising probes both for the study of the in-medium properties of hadrons and the nuclear equation-of-state. According to calculations, the effective mass of a K^+-meson increases moderately with increasing baryon density whereas the effective mass of K^--mesons decreases significantly (see *e.g.* [3,4,6]). In mean-field calculations, this effect is caused by a repulsive K^+N potential and an attractive K^-N potential. It has been speculated [5] that an attractive K^-N potential will lead to Bose condensation of K^--mesons in the core of neutron stars above baryon densities of about 3 times saturation density (*cf.* "nucleon star" model in Fig. 1). Microscopic calculations predict a dynamical broadening of the K^--meson spectral function which is shifted towards smaller energies [7,8]. The ultimate goal is to relate the in-medium spectral function of kaons and antikaons to the anticipated chiral symmetry restoration at high baryon density.

Experiments on kaon and antikaon production and propagation in heavy-ion collisions at relativistic energies have been performed with the Kaon Spectrometer and the FOPI detector at the heavy-ion synchrotron SIS at GSI Darmstadt. Recent results are published in [9–14].

In order to see indications for in-medium effects on K^+ and K^- production we compare nucleus–nucleus to proton–proton collisions. Fig. 3 shows the multiplicity of K^+- and K^--mesons per average number of participat-

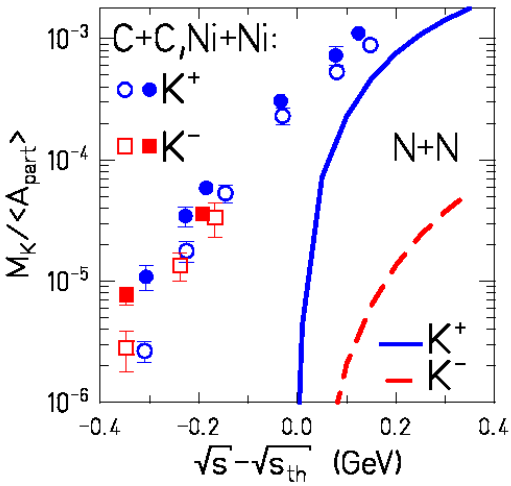

Fig. 3. K^+ (circles) and antikaon (squares) multiplicity per participating nucleon as a function of the Q-value for C+C (open symbols) and Ni+Ni (full symbols) collisions [11,13,15]. The lines correspond to parameterisations of the production cross sections for K^+ (solid) and K^- (dashed) in nucleon–nucleon collisions [16–18].

ing nucleons $M_K/\langle A_{\rm part}\rangle$ as function of the Q-value in the NN system. The data were measured in C+C and Ni+Ni collisions by the KaoS Collaboration [11, 13, 15]. The lines represent parameterisations of the available proton–proton data averaged over the isospin channels [16–18]. In nucleon–nucleon collisions the kaon multiplicity exceeds the antikaon multiplicity by 1–2 orders of magnitudes at the same Q-value. This large difference has disappeared for nucleus–nucleus collisions where the kaon and antikaon data nearly fall on the same curve. This observation demonstrates that in nucleus–nucleus collisions the production of antikaons is much more enhanced than the production of kaons. Within transport calculations, the K^- yield enhancement is explained by two effects: *(i)* strangeness exchange reactions such as $\pi\Lambda \to K^-N$ and *(ii)* a reduced effective K^- mass in dense nuclear matter [6].

A comparison of experimental data to results of transport calculations is presented in Fig. 4. The figure shows the K^+ and K^- multiplicity densities dN/dy and their ratio for near-central Ni+Ni collisions at 1.93 AGeV as function of the rapidity $y_{\rm CM}$. The rapidity is defined here as $y_{\rm CM} = y - 0.5 \times y_{\rm proj}$.

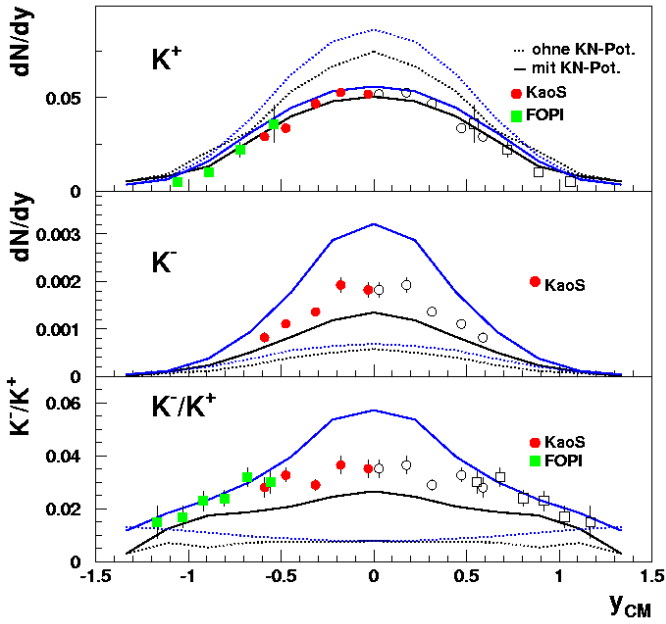

Fig. 4. Multiplicity density distributions of K^+ (upper panel) and K^--mesons (center panel) for near-central (b < 4.4 fm) Ni+Ni collisions at 1.93 AGeV. Circles: KaoS data [13], squares: FOPI data [9, 19]. The measured data (full symbols) are mirrored at $y_{\rm CM}$=0 (open symbols). Lower panel: K^-/K^+ ratio. The data are compared to BUU transport calculations. Solid lines: with in-medium effects. Dotted lines: without in-medium effects. Calculation [6] is always above [20].

The value $y_{CM} = 0$ corresponds to mid-rapidity and $y_{CM} = v \pm 0.89$ to projectile or target rapidity, respectively. Fig. 4 combines data measured by the KaoS Collaboration (circles) [13] and by the FOPI Collaboration (squares) [9,19].

The data are compared to results of RBUU transport calculations performed by Li and Brown (grey lines [20]) and Cassing and Bratkovskaya (black lines [6]). The dashed lines represent the results of calculations with bare kaon and antikaon masses whereas the solid lines are calculated with in-medium masses. The "bare mass" calculations clearly overestimate the K^+ yield and underestimate the K^- yield. The results of the "in-medium" calculations reproduce well the K^+ data but not the K^- data which are overestimated by Li and Brown and underestimated by Cassing and Bratkovskaya. The data allow for a fine tuning of the strength of the K^-N potential which is a free parameter in those models.

Another observable consequence of in-medium KN potentials is their influence on the propagation of kaons and antikaons in heavy-ion collisions. The measured azimuthal emission patterns of K^+-mesons, which cannot be absorbed as they contain an antistrange quark, contradict the naive picture of a long mean free path in nuclear matter. The particular feature of sideward flow [12] and the pronounced out-of-plane emission around mid-rapidity [10] indicate that K^+-mesons are repelled from the regions of increased baryonic density as expected for a repulsive K^+N potential [21,22]. The azimuthal angle distribution of K^+-mesons from Au+Au collisions at a beam energy of 1 AGeV is shown in Fig. 5. The data (full symbols) [10] are compared to results of a QMD transport calculation with (open circles) and without (open squares) K^+N potential [22].

The key observable is the azimuthal emission pattern of K^--mesons. If an attractive K^-N potential exists as suggested by the measured K^- yields, the K^--mesons will be emitted isotropically in semi-central Au+Au collisions [22]. This observation would be in contrast to the behaviour of pions and K^+-mesons and hence would provide strong experimental evidence for in-medium modifications of antikaons. Such an experiment has been performed by the KaoS Collaboration. The analysis is in progress.

Once the in-medium properties of kaons are under control, one can attack an old problem of nuclear physics which is the determination of the nuclear equation of state. The idea is that the production of K^+-mesons in collisions between very heavy nuclei at subthreshold beam energies is sensitive to the baryon density. The density reached in the fireball depends on the nuclear compressibility. Recent measurements of the K^+ production excitation function in Au+Au and, as a reference system, in C+C collisions provide evidence for a soft nuclear equation of state [14,23].

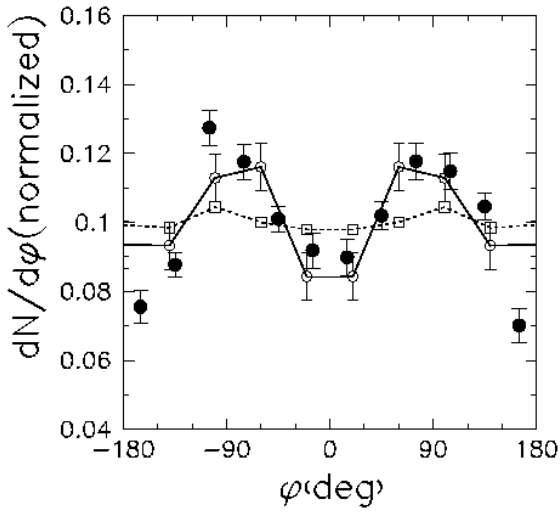

Fig. 5. K^+ azimuthal angle distribution for semi-central Au+Au collisions at 1 AGeV. The data (full dots) are measured in the rapidity range $0.2 \leq y/y_{\mathrm{proj}} \leq 0.8$ [10]. The open symbols and the lines respresent results of a QMD transport calculation [22] with repulsive K^+N potential (open circles, full line) and without K^+N potential (open squares, dashed line).

3. Future experiments at high baryon densities

Experiments at the CERN–SPS have studied high-energy heavy-ion collisions in order to explore the QCD phase diagram in the region of high temperatures and low baryon densities. In nature such extreme conditions were reached in the early universe, a few microseconds after the Big Bang. Experiments at RHIC and at the future LHC will continue this way and investigate the quark–gluon plasma at vanishing net baryon density (see Fig. 6).

The major goal of the nuclear reaction experiment at the future GSI facility is to explore the presently almost unknown region of high baryon densities in the phase diagram of strongly interacting matter. The territory of dense baryonic matter accessible in heavy-ion collisions is located between the line of chemical freeze-out and the hadron/parton phase boundary, as indicated by the hatched area in Fig. 6. Moreover, new states of matter beyond the deconfinement and chiral transition at high net baryon densities and moderate temperatures may be within the reach of the experiment. A particular challenge for future heavy-ion experiments is the search for the predicted "critical point" in the phase diagram of strongly interacting matter. Pioneering experiments which investigated hadronic observables in the energy range from 2 to about 15 AGeV have been performed at

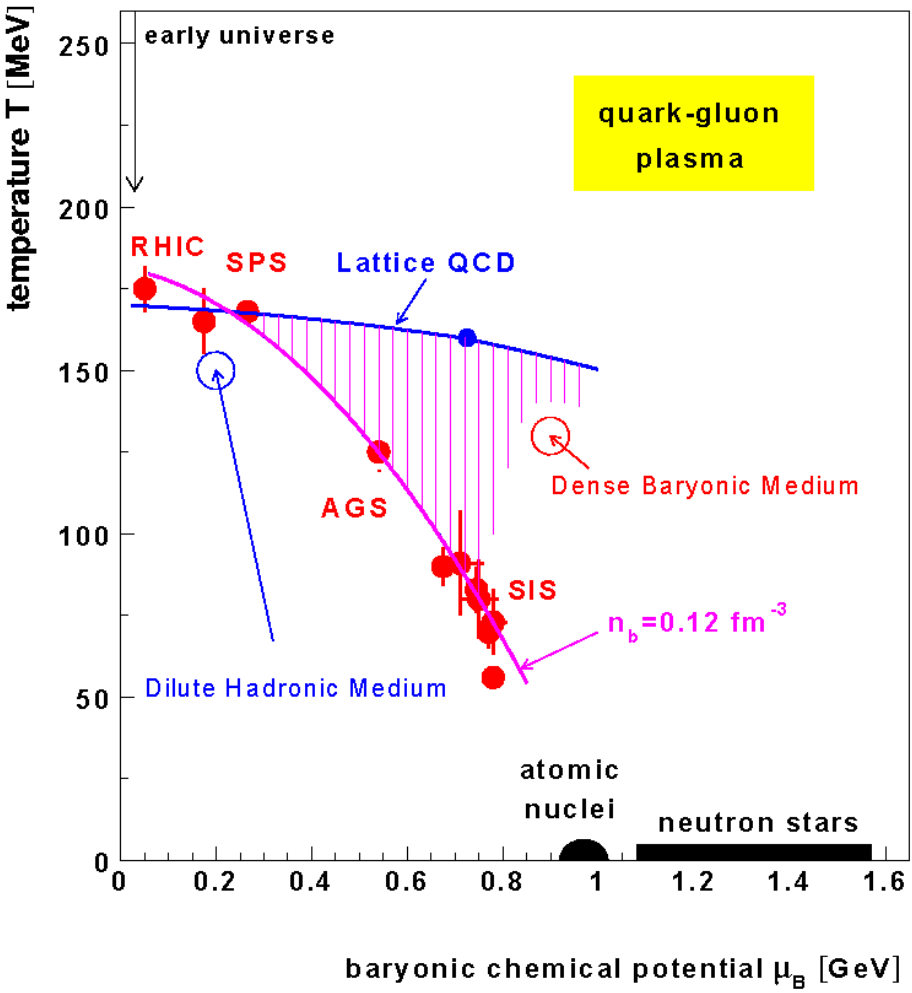

Fig. 6. The phase diagram of strongly interacting matter. The symbols represent freeze-out points obtained with a statistical model analysis from particle ratios measured in heavy collisions [24–26]. The curve through the data points refers to a calculation of the chemical freeze-out which occurs at a constant baryon density of $\rho_B = 0.75\ \rho_0$ (with $\rho_0 = 0.16\,\mathrm{fm}^{-3}$). The curve labelled "Lattice QCD" represents the phase boundary as obtained with a QCD lattice calculation [28] with a critical point (full dot) at $T = 160 \pm 3.5$ MeV and $\mu_B = 725 \pm 35$ MeV ($\rho_B \approx 3\rho_0$). In the region of the circle labelled "dilute hadronic medium" the baryon density is $\rho_B = 0.038\,\mathrm{fm}^{-3} \approx 0.24\rho_0$. The corresponding value for the other circle ("dense baryonic medium") is $\rho_B = 1.0\,\mathrm{fm}^{-3} \approx 6.2\rho_0$. The hatched area marks the region of equilibrated matter at high baryon densities.

the AGS in Brookhaven. Fig. 6 presents a calculated chemical freeze-out curve and the freeze-out points (full dots) as derived from particle production data obtained at SIS, AGS, SPS and RHIC [24–27]. The baryon density at freeze-out corresponds to a value of 0.75 ρ_0. The curve labelled "Lattice QCD" represents the phase boundary as predicted by a recent QCD lattice calculation for finite baryon chemical potential [28]. According to the calculations, the phase boundary and the freeze-out curve merge at small baryon chemical potentials ($\mu_B \leq$ 200–300 MeV). The SPS and RHIC data suggest that, at ultra-relativistic beam energies, hadronization and freeze-out occurs almost simultaneously (which implies that the fireball was born into the quark–gluon phase).

The QCD lattice calculation predicts a critical point at a temperature of 160 ± 3.5 MeV and a chemical potential of 725 ± 35 MeV (corresponding to a baryon density of about $3\,\rho$). The critical point is located not too far from the AGS freeze-out point and hence could be reached with the future GSI accelerator. The discovery of the critical point would represent a major progress in the exploration of the QCD phase diagram [29].

With the proposed experimental setup one will be able to measure the observables discussed above in nucleus–nucleus collisions at beam energies between 2 and 30 AGeV. The energy range from 2 to 7 AGeV will be covered by the (slightly modified) HADES detector whereas the new Compressed Baryonic Matter (CBM) experiment is designed for the energy range from 7 to 40 AGeV. The envisaged physics program includes:

- search for signatures of chiral symmetry restoration in dense baryonic matter. Probes: Dilepton pairs from light vector mesons, the yield of open charm (D-mesons) and the ratio of open to hidden charm;
- search for signatures of the deconfinement phase transition at large baryonic chemical potentials. Probes: charmonium, strangeness, collective flow;
- search for the critical point. Probes: event-by-event fluctuations of hadronic observables (K/π ratio, average transverse momentum of hadrons);
- search for exotic states of matter such as condensates of strange particles or color superconductivity. Probes: strange and multistrange particles, K/π ratio.

The interest in heavy ion collisions at beam energies around 30 AGeV was enhanced by recent results of experiments on strangeness production [30,31] as shown in Fig. 7. It was observed that the kaon-to-pion yield ratio

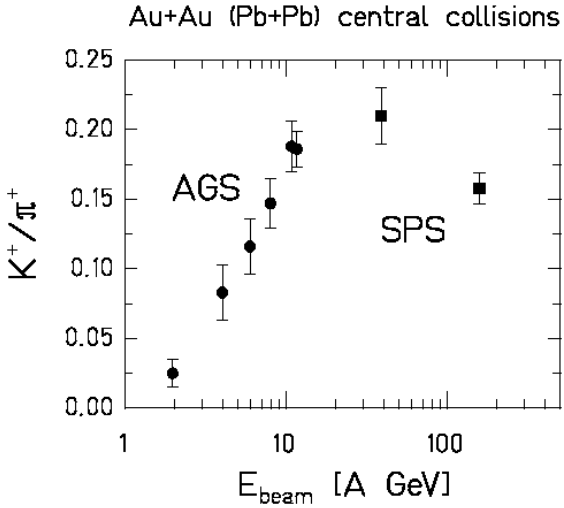

Fig. 7. K^+/π^+ ratio measured in central Au+Au (Pb+Pb) collisions as function of bombarding energy. AGS data [30], SPS data [31].

(K^+/π^+) measured in central Au+Au (Pb+Pb) collisions exhibits a maximum in the beam energy range between about 20 and 40 AGeV. This relative maximum of the strangeness content has been attributed to the enhanced production of strange quarks (and antiquarks) in the deconfined phase [32]. On the other hand, a maximum of the ratio of strange to nonstrange particle production is predicted for beam energies around 30 AGeV by a statistical model calculation without assuming a phase transition [33]. This maximum is unique to heavy ion collisions, and has no equivalent in collisions between elementary particles. The model calculations indicate that the distinct maximum of the ratio of strange to nonstrange particles around 30 AGeV is dominantly caused by the relative abundance of strange baryons.

The data on the K^+/π^+ ratio and their interpretations indicate that "strange" conditions exist inside the fireball as created in heavy ion collisions around 30 AGeV. Future detailed experimental studies of nucleus–nucleus reactions in this energy range, in particular the production of multistrange hyperons ($\Xi, \bar{\Xi}, \Omega, \bar{\Omega}$), will help to unravel the role of strangeness at high baryon densities. The observation of mesons containing charm quarks is of particular importance. Due to the large mass of charm quarks, a charm–anticharm pair can be produced only in a hard collision between two quarks or two gluons. Hence charmed mesons are messengers from the early fireball — created prior to expansion and freezeout. For central lead–lead collisions an anomalous suppression of J/ψ mesons has been observed at SPS ener-

gies [35]. This effect was predicted and interpreted as screening of $c\bar{c}$ pairs in the quark phase [36]. Most of the created charm quarks, however, are confined in D-mesons together with a light quark. Therefore, the observation of open charm in heavy ion collisions is of crucial importance for the interpretation of signatures of a possible deconfinement phase transition. So far D-mesons have not been observed in nucleus–nucleus collisions.

Charm production (both J/ψ and D-mesons) will be also an important probe for the high baryon density regime of the QCD phase diagram. In particular at beam energies close to threshold, charm production might depend on the conditions inside the dense fireball. The charmonium yield, measured as function of collision centrality, will be sensitive to a possible deconfinement phase transition. The measurement of open charm provides the unique possibility to study in-medium properties of hadrons at very high baryonic densities. The effective masses of D-mesons, which consist of a heavy charm quark and a light quark, are expected to be modified substantially in dense matter, in a way analogous to the masses of K-mesons [37,38]). The production thresholds in proton–proton (or proton–neutron) collisions are 11.3 GeV for J/ψ mesons, 11.9 GeV for D-mesons and 14.9 GeV for Anti-D-mesons. Fig. 8 shows multiplicities of J/ψ, D-mesons and lighter mesons produced in central Au+Au collisions as function of beam energy as calculated with the HSD transport model [39].

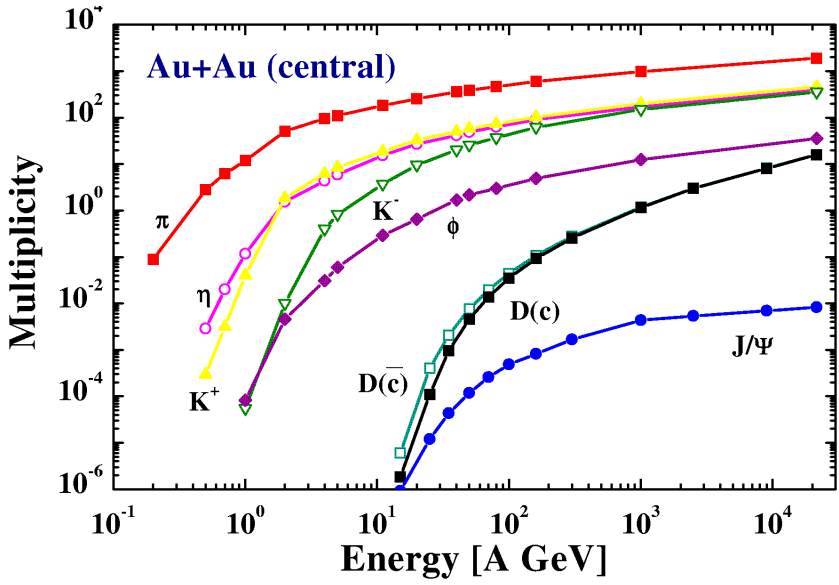

Fig. 8. Multiplicities of mesons produced in central Au+Au collisions as function of beam energy according to the HSD transport code [39].

The (partial) restoration of chiral symmetry is expected to modify the in-medium spectral function of short lived vector mesons like the ρ-meson. This effect is studied experimentally by measuring the decay of a ρ-meson into a pair of leptons which are not disturbed by interaction with the fireball matter. An enhanced yield of electron–positron pairs in the low mass region of the invariant mass spectrum has been observed in central lead-lead collisions at 158 AGeV [40]. It is still under debate whether this enhancement is caused by a shift and/or a broadening of the ρ-meson spectral function or by thermal radiation from the quark–gluon plasma [41].

No dilepton experiment has been performed so far in the beam energy range between AGS and CERN–SPS. We propose to measure the leptonic decay of light vector mesons (ρ-, ω- and ϕ-mesons) at beam energies between 5 and 30 AGeV. These data will shed light on the fundamental question to what extend chiral symmetry is restored at high baryon densities and how this affects hadron masses.

A simultaneous measurement of charmonium, D-mesons, multistrange hyperons and light vector mesons (together with protons, pions and kaons) in one single experiment has not been performed up to now. Such an experiment permits to study the behavior of different probes and their correlations under identical experimental conditions (such as impact parameter selection). An intriguing idea is to investigate collisions between deformed uranium nuclei and to select those events where the two nuclei collided tip-on-tip. In such a collision the baryonic density is increased by about 30 % (with respect to a collision between two spherical nuclei) and the reaction time is extended by almost a factor of 2 [42].

4. The Compressed Baryonic Matter (CBM) experiment

We propose to build a universal instrument which will be able to measure both leptons and hadrons and to identify efficiently rare probes in a large background of charged particles. The experimental challenge is the large track density of charged particles in central Au+Au collisions at 25 AGeV. According to the URQMD event generator [43] such an event consists of about 160 protons, 800 charged pions and 60 kaons (K^+ and K^-). Based on these simulations we have designed the experimental setup. It turns out that the apparatus described below accepts about 80% of the protons, 60% of the kaons (including decay in flight), 67 % of the pions, 20% of J/ψ mesons and 30 % of the D-mesons (branching ratios for the decays $J/\psi \to e^+e^-$ and $D \to K\pi\pi$ not included).

The experiment combines state-of-the-art detector components which in part are under development for future experiments at the Large Hadron Collider at CERN: large arrays of radiation hard silicon pixel (and strip)

detectors for precise tracking and vertex reconstruction, transition radiation detectors and ring-imaging Cherenkov detectors for electron identification and resistive-plate-chamber arrays for time-of-flight measurements.

The proposed experimental setup (see Fig. 9) consists of the following components:

- Dipole magnet.

  The magnetic field bends the particles according to their momentum (and charge) and prevents most of the abundantly produced δ-electrons from hitting the detectors.

- Radiation hard Silicon pixel/strip detectors.

  A set of Silicon pixel (and strip) detectors close to the target allow to determine the particle trajectory (and hence the momentum) with high accuracy. This Silicon tracker will measure the decay topology of hyperons and hence their invariant mass. A vertex resolution of better than 50 μm is required for the identification of charmed mesons.

- Transition radiation detector (TRD).

  The TRD allows to identify high energy electrons ($\gamma > 2000$) and hence the measurement of charmonium via the invariant mass of the electron–positron pair.

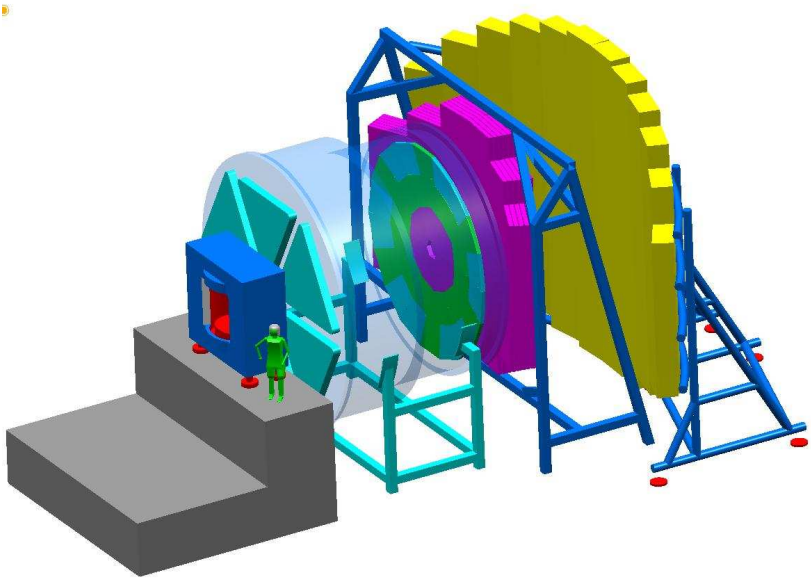

Fig. 9. Sketch of the experimental setup (see text).

- Ring imaging Cherenkov detector (RICH).

  The RICH detector provides identification of electrons with $\gamma > 40$ corresponding to the momentum range of di-electrons from decaying ρ-mesons. When using a radiator with higher refractive index the RICH signals can be used to identify high energy pions and kaons.

- TOF stop wall: resistive plate counters (RPC).

  The large area RPC provides the stop signal for the time-of-flight measurement which allows the identification of low momentum particles. A TOF distance of 10 m results in a time difference of 400 ps for pions and kaons of 3 GeV/c momentum.

- TOF start detector.

  A Diamond pixel detector provides the start signal for the TOF measurement. It will count directly the beam particles up to intensities of 10^9 ions/sec.

The Compressed Baryonic Matter (CBM) experiment is part of a proposal for a new accelerator facility at GSI in Darmstadt (see also the contribution of V. Metag).

The data on strangeness production presented in this paper were measured and analyzed by my colleagues of the KaoS Collaboration: I. Böttcher, A. Förster, E. Grosse, P. Koczoń, B. Kohlmeyer, M. Menzel, L. Naumann, H. Oeschler, E. Schwab, W. Scheinast, Y. Shin, H. Ströbele, C. Sturm, F. Uhlig, A. Wagner and W. Waluś. The conceptual design study of the compressed baryon matter experiment is performed by a working group which actually consists of A. Andronic, P. Braun-Munzinger, C. Finck, B. Friman, N. Herrmann, R. Holzmann, W. König, M. Lutz, P.S., Y. Shin, R. Simon, H. Ströbele and J. Stroth.

REFERENCES

[1] F. Weber, *J. Phys. G; Nucl. Part. Phys.* **27**, 465 (2001).
[2] B. Friman, W. Nörenberg, V.D. Toneev, *Eur. Phys. J.* **A3**, 165 (1998).
[3] G.E. Brown *et al.*, *Phys. Rev.* **C43**, 1881 (1991).
[4] J. Schaffner-Bielich *et al.*, Nucl. Phys. **A625**, 325 (1997).
[5] G.Q. Li, C.H. Lee, G.E. Brown, *Phys. Rev. Lett.* **79**, 5214 (1997).
[6] W. Cassing, E. Bratkovskaya, *Phys. Rep.* **308**, 65 (1999).

[7] T. Waas, N. Kaiser, W. Weise, *Phys. Lett.* **B379**, 34 (1996).
[8] M. Lutz, *Phys. Lett.* **B426**, 12 (1998).
[9] D. Best *et al.*, *Nucl. Phys.* **A625**, 307 (1997).
[10] Y. Shin *et al.*, *Phys. Rev. Lett.* **81**, 1576 (1998).
[11] F. Laue, C. Sturm *et al.*, *Phys. Rev. Lett.* **82**, 1640 (1999).
[12] P. Crochet *et al.*, *Phys. Lett.* **B486**, 6 (2000).
[13] M. Menzel *et al.*, *Phys. Lett.* **B495**, 26 (2000).
[14] C. Sturm *et al.*, *Phys. Rev. Lett.* **86**, 39 (2001).
[15] R. Barth *et al.*, *Phys. Rev. Lett.* **78**, 4007 (1997).
[16] A. Sibirtsev, *Phys. Lett.* **B359**, 29 (1995).
[17] E. Bratkovskaya, W. Cassing, U. Mosel, *Nucl. Phys.* **A622**, 593 (1997).
[18] A. Sibirtsev, W. Cassing, C.M. Ko, *Z. Phys.* **A358**, 101 (1997).
[19] K. Wisniewski *et al.*, *Eur. Phys. J.* **A9**, 515 (2000).
[20] G.Q. Li, G.E. Brown, *Phys. Rev.* **C58**, 1698 (1998).
[21] G.Q. Li, C.M. Ko, G.E. Brown, *Phys. Lett.* **B381**, 17 (1996).
[22] Z.S. Wang *et al.*, *Eur. Phys. J.* **A5**, 275 (1999).
[23] C. Fuchs *et al.*, *Phys. Rev. Lett.* **86**, 1974 (2001).
[24] R. Stock, *Phys. Lett.* **B456**, 277 (1999).
[25] P. Braun-Munzinger, I. Heppe, J. Stachel, *Phys. Lett.* **B465**, 15 (1999).
[26] J. Cleymans, K. Redlich, *Phys. Rev. Lett.* **81**, 5284 (1998).
[27] P. Braun-Munzinger, *Nucl. Phys.* **A681**, 119c (2001).
[28] Z. Fodor, S.D. Katz, `hep-lat/0106002`.
[29] K. Rajagopal, *Nucl. Phys.* **A661**, 150c (1999).
[30] L. Ahle *et al.*, *Phys. Rev.* **C58**, 3523 (1998); *Phys. Lett.* **B476**, 1 (2000); *Phys. Lett.* **B490**, 53 (2000).
[31] J. Bächler *et al.*, *Nucl. Phys.* **A661**, 45c (1999); H. Ströbele, private communication.
[32] M. Gazdzicki, M. Gorenstein, D. Röhrich, `hep-ph/0006236`.
[33] P. Braun-Munzinger *et al.*, `hep-ph/0106066`.
[34] J. Cleymans, K. Redlich, *Phys. Rev.* **C60**, 054908 (1999).
[35] M. Abreu *et al.*, *Phys. Lett.* **B477**, 28 (2000).
[36] T. Matsui, H. Satz, *Phys. Lett.* **B178**, 416 (1986).
[37] W. Weise *et al.* Proccidings of the workshop "Hadrons in Matter", Hirschegg, Austria 2001.
[38] A. Sibirtsev, K. Tsushima, A.W. Thomas, *Eur. Phys. J.* **A6**, 351 (1999).
[39] W. Cassing, E. Bratkovskaya, A. Sibirtsev, `nucl-th/0010071`.
[40] G. Agakichiev *et al.*, *Phys. Lett.* **B422**, 405 (1998).
[41] R. Rapp, *Nucl. Phys.* **A661**, 33c (1999).
[42] Bao-An Li, *Phys. Rev.* **C61**, 021903 (2000).
[43] S.A. Bass *et al.*, *Prog. Part. Nucl. Phys.* **41**, 225 (1998).